

## **PIEZOCERAMIC TRANSDUCER FOR ULTRASONIC SHEAR WAVE EXCITATION – MODELLING AND NUMERICAL SIMULATIONS**

**EMIL ALEKSIEWICZ-DRAB, ALEKSANDRA ZIAJA-SUJDAK, RAFAŁ RADECKI,  
MARIUSZ OSIKA AND WIESLAW J. STASZEWSKI**

Department of Robotics and Mechatronics  
AGH University of Science and Technology  
Al. Mickiewicza 30, 30-059 Krakow, Poland  
e-mail: rafal.radecki@agh.edu.pl

**Abstract.** The fundamental shear horizontal wave is attractive for structural damage detection due to its non-dispersive property. However, in contrast to longitudinal ultrasonic waves, excitation of shear waves is always a challenge. A thickness-shear  $d_{15}$  piezoceramic transducers is modelled using finite elements. The major focus is on the excitability and directivity of the SH0 mode. The results show that the geometry of the transducer significantly affects the generation of the fundamental shear horizontal mode in the plate.

**Key words:** Shear Horizontal Wave Excitation, Piezoceramic Transducers, Finite Element Modelling, Numerical Simulations,

### **1 INTRODUCTION**

Structural health monitoring relies on different methods that are used for damage detection in large structures. Damage detection methods based on ultrasonic waves and low-profile piezoceramic transducers - that can be surface-bonded to monitored structures - are attractive for engineering applications, particularly in aerospace industries. Lamb waves have been investigated in this research area for decades. Various monitoring strategies, damage detection methods and excitation techniques have been developed in this field, as reviewed in [1-3]. Recent years have brought more attention to ultrasonic shear horizontal waves [5-6]. The fundamental shear horizontal (SH0) wave is particularly attractive due to its non-dispersive property and sensitivity to small defects. The latter benefit often involves nonlinear wavefield [6-7]. However, in contrast to longitudinal ultrasonic waves, excitation of shear waves is always a challenge. Various technologies can be used for the excitation of shear waves [8]. These technologies are based mainly the magnetostrictive [9] and piezoelectric effects [10]. The magnetostrictive effect is utilised in the Electro-Magnetic Acoustic Transducers (EMATs). The piezoelectric effect is used in piezoelectric bulk probes and in piezoceramic transducers. The latter transducers are low-profile, can be easily surface-bonded and therefore are particularly attractive for excitation and sensing of shear waves. These transducers can

work in face- [11] and thickness-shear modes [12]. Although the former transducers are better for pure shear mode excitation and offer better generation/reception properties, the latter are more suitable for phase array systems based on omnidirectional shear waves.

The paper investigates a  $d_{15}$  thickness-shear piezoceramic square transducer. The major focus is on generation property and directivity of SH0 shear waves. Section 2 describes a simple model of the analysed piezoceramic transducer. Finite elements are used to build the model. Numerical simulation results are given in Section 3. The paper is concluded in Section 4. The results show that the geometry of the transducer significantly affects the generation of SH0 mode in the plate.

## 2 PIEZOCERAMIC TRANSDUCER MODEL FOR SHEAR WAVE EXCITATION

This section describes the model of the  $d_{15}$  thickness-shear piezoceramic transducer. Firstly, some basic theoretical background related to shear wave excitation and piezoelectricity is provided. Then a finite element model of the analysed transducers is described.

### 2.1 Shear horizontal waves

Shear waves exhibit particle motion that is perpendicular to wave direction. These waves can be polarised horizontally (SH waves) and vertically (SV waves). The fundamental mode (SH0) of the former wave is particularly attractive for structural damage detection due to its non-dispersive nature. The SH0 particle motion can be described by the following wave equation [13,14]

$$\frac{\partial^2 u_3}{\partial x_1^2} + \frac{\partial^2 u_3}{\partial x_2^2} = \frac{1}{c_T^2} \frac{\partial^2 u_3}{\partial t^2}, \quad (1)$$

where  $u_3(x_1, x_2, t)$  is the only non-zero displacement and  $c_T$  is the shear wave speed. The particle displacement can be expressed as

$$u_3(x_1, x_2, t) = f(y)e^{i(kx - \omega t)}, \quad (2)$$

where  $\omega$  is the circular frequency and  $k$  is the wave number. When Equation (2) is introduced to Equation (1), the general form of the displacement field can be given as

$$u_3(x_1, x_2, t) = [A \sin(qx_2) + B \cos(qx_2)]e^{i(kx_1 - \omega t)} \quad (3)$$

where  $q = \sqrt{\omega^2/c_T^2 - k^2}$  and  $A, B$  are arbitrary constants. The displacement field given by Equation (3) can be separated into symmetric and antisymmetric components. When the relevant boundary conditions can be imposed on the displacement motion, the dispersion

equations can be obtained. Since the non-dispersive SH0 mode is of interest in this paper, these equations are not analysed.

## 2.2 Piezoelectric equations – theoretical background

The piezoelectric effect – that can be observed in piezoceramic materials - results from the cross coupling of the mechanical and electrical fields. This coupling can be described by the following equations [15]

$$\begin{aligned}\{S\} &= [s^E]\{T\} + [d^t]\{E\} \\ \{D\} &= [d]\{T\} + [\varepsilon^T]\{E\}\end{aligned}\tag{4}$$

where  $S$  is the strain tensor,  $D$  is the electric flux density tensor,  $T$  is stress tensor,  $E$  is the electric field strength tensor,  $\varepsilon$  the permittivity,  $s$  is the compliance under short-circuit condition,  $d$  and  $d^t$  are the matrices for the direct and converse piezoelectric effect, respectively. The superscripts T and E in the above equations stand for the zero or constant stress and electric field, respectively. The tensor directions are defined in Figure 1. Here, “1”, “2” and “3” denote the longitudinal, transverse and thickness direction, respectively, and the shear planes re depicted by the subscripts “4”, “5” and “6”.

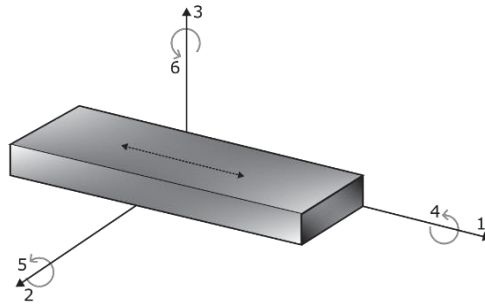


**Figure 1:** Definitions of tensor directions used in the constitutive electro-mechanical equations.

With the direction used in Figure 1 - when the PZT-5J material considered in this paper is used - Equation (4) can be expanded as

$$\begin{bmatrix} s_1 \\ s_2 \\ s_3 \\ s_4 \\ s_5 \\ s_6 \end{bmatrix} = \begin{bmatrix} s_{11}^E & s_{12}^E & s_{13}^E & 0 & 0 & 0 \\ s_{21}^E & s_{22}^E & s_{23}^E & 0 & 0 & 0 \\ s_{31}^E & s_{32}^E & s_{33}^E & 0 & 0 & 0 \\ 0 & 0 & 0 & s_{44}^E & 0 & 0 \\ 0 & 0 & 0 & 0 & s_{55}^E & 0 \\ 0 & 0 & 0 & 0 & 0 & s_{66}^E \end{bmatrix} \begin{bmatrix} T_1 \\ T_2 \\ T_3 \\ T_4 \\ T_5 \\ T_6 \end{bmatrix} + \begin{bmatrix} 0 & 0 & d_{13} \\ 0 & 0 & d_{23} \\ 0 & 0 & d_{33} \\ 0 & d_{42} & 0 \\ d_{51} & 0 & 0 \\ 0 & 0 & 0 \end{bmatrix} \begin{bmatrix} E_1 \\ E_2 \\ E_3 \end{bmatrix} \quad (5)$$

$$\begin{bmatrix} D_1 \\ D_2 \\ D_3 \end{bmatrix} = \begin{bmatrix} 0 & 0 & 0 & 0 & d_{15} & 0 \\ 0 & 0 & 0 & d_{24} & 0 & 0 \\ d_{31} & d_{32} & d_{33} & 0 & 0 & 0 \end{bmatrix} \begin{bmatrix} T_1 \\ T_2 \\ T_3 \\ T_4 \\ T_5 \\ T_6 \end{bmatrix} + \begin{bmatrix} \varepsilon_{11}^T & 0 & 0 \\ \varepsilon_{21}^T & \varepsilon_{22}^T & 0 \\ 0 & 0 & \varepsilon_{33}^T \end{bmatrix} \begin{bmatrix} E_1 \\ E_2 \\ E_3 \end{bmatrix}$$

This clearly explains how the piezoelectric material behaves. For the  $d_{15}$  mode used, the electric field can be applied either along or through the thickness of the transducer. The former excitation is considered in the paper.

### 2.3 Directivity of wave propagation - finite element model

Shear wave generation in a  $400 \times 400 \times 2$  mm glass plate has been investigated using the *ABAQUS* finite elements software. The plate has been modelled using the following material properties: density  $\rho = 2616 \text{ kg/m}^3$ , Young's modulus  $E = 60.547 \text{ GPa}$  and Poisson's ratio  $\nu = 0.212$ . The  $6 \times 6 \times 2.5$  mm surface-bonded piezoceramic transducer - working in the  $d_{15}$  mode - has been used initially for shear wave excitation. The electric field has been supplied along the thickness of the transducer. The 10-cycle sine burst – enveloped by the Hanning window – has been used as the excitation signal. The amplitude of excitation has been equal to  $100 \text{ V}_{pp}$ . The SM411 material properties – equivalent to PZT-5J – have been used to model the transducer [16]. The time step of  $10^{-8} \text{ s}$  and element size of  $0.5 \text{ mm}$  have been selected to guarantee numerical stability.

The excitation in the plate leads not only to shear wave but also to Lamb wave generation. However, since the directivity of the transducer has been of interest, the transducer has been geometrically optimised to maximise the amplitude of the SH0 mode. There are two important parameters that control guided wave excitation. The first one is the ratio of transducer dimension  $d$  in the direction of mode propagation to its wavelength  $\lambda$ . This ratio controls the energy level under transduction are of the transducer as a function of frequency for a given mode. Resonance frequencies, which are characterised by maximum amplitudes can be obtained for wavelengths that satisfies the following equation

$$\frac{n\lambda}{2} = d \quad (6)$$

where  $n = 1, 2, 3, \dots$ . The second parameter is the ratio of the propagating mode wavelength to the transducer's dimension perpendicular to the propagating axis. This ratio controls the aperture and the number of generated lobes. From the far-field wave propagation theory, if the ratio  $\lambda/d$  is greater than or equal to one, the excitation source acts as a dipole, i.e., the main lobe only appears. On the other hand, if this ratio is less than one, the aperture reduces, and side lobes of smaller amplitude appear. Therefore, in order to generate the SH0 mode, the length of the transducer should be greater than - or at least equal to - the wavelength of the propagating SH0 mode. One should note that due to the square shape of the modelled transducer, only the SH0 mode generation has been maximised (i.e., the effect of Lamb wave generation has not been minimised).

Two different excitation frequencies – i.e., 220 and 617.5 kHz - has been used to demonstrate the directivity of wave propagation. In order to obtain the wave generation directivity pattern, an array of 91 sensors - placed on a circle of 100 mm diameter – has been used, as illustrated in Figure 2. These sensors have been spaced by  $1^\circ$ . One should note that the quarter of the circle is sufficient to obtain the full directivity pattern due to the symmetric (and antisymmetric) property of SH0 shear wave propagation.

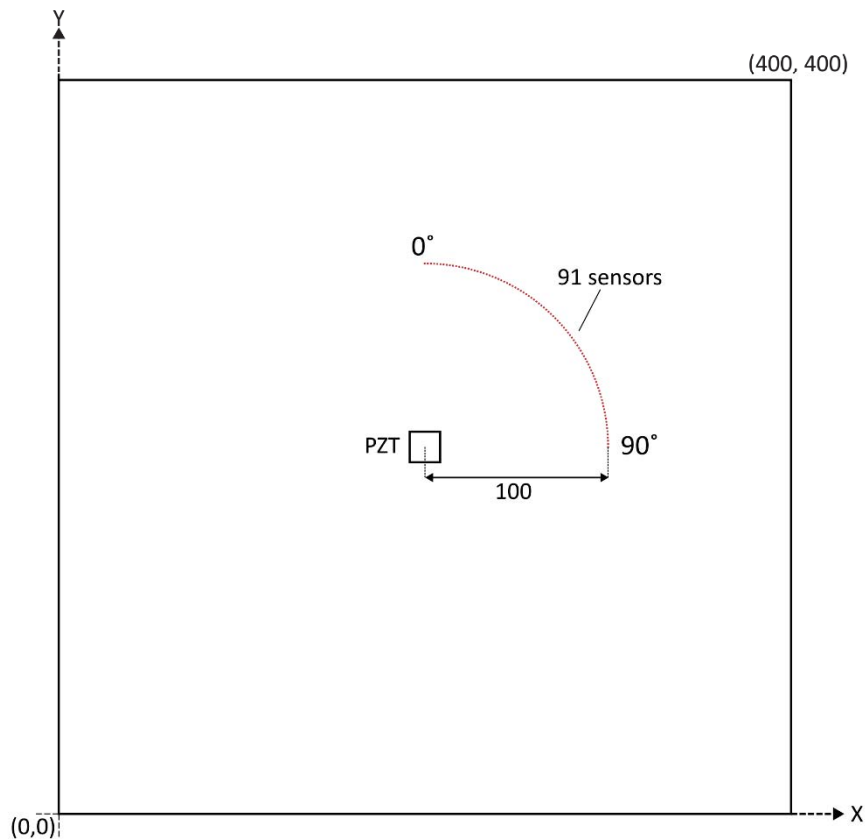


**Figure 2:** Plate model used for the directivity study of shear wave propagation. The excitation transducer is in the centre of the plate. The sensors are positions on a quarter of the indicated circle.

Maximum values of velocity have been gathered from wave responses corresponding to different sensor locations. Then in-plane velocity components have been transformed into the radial and tangential components, as explained in [10]. These calculations have been performed using MATLAB. The radial, tangential and the out-of-plane component correspond to the SH0 shear horizontal wave mode, S0 and A0 Lamb wave modes, respectively.

### 3 NUMERICAL SIMULATION RESULTS

Once the piezoceramic transducer has been excited, wave propagation responses have been gathered, following the procedure described in Section 2.3. The dispersion curves have been used to identify wave propagation modes. Figure 3 gives an example of collected wave responses. The SH0, S0 and A0 wave modes can be clearly observed. One should note different amplitudes of wave responses. The amplitude of the shear horizontal SH0 mode is larger than the amplitude of the Lamb wave modes. The solid red lines indicate the relevant envelopes calculated using the Hilbert transform. Wave global maxima are indicated using a red circle.

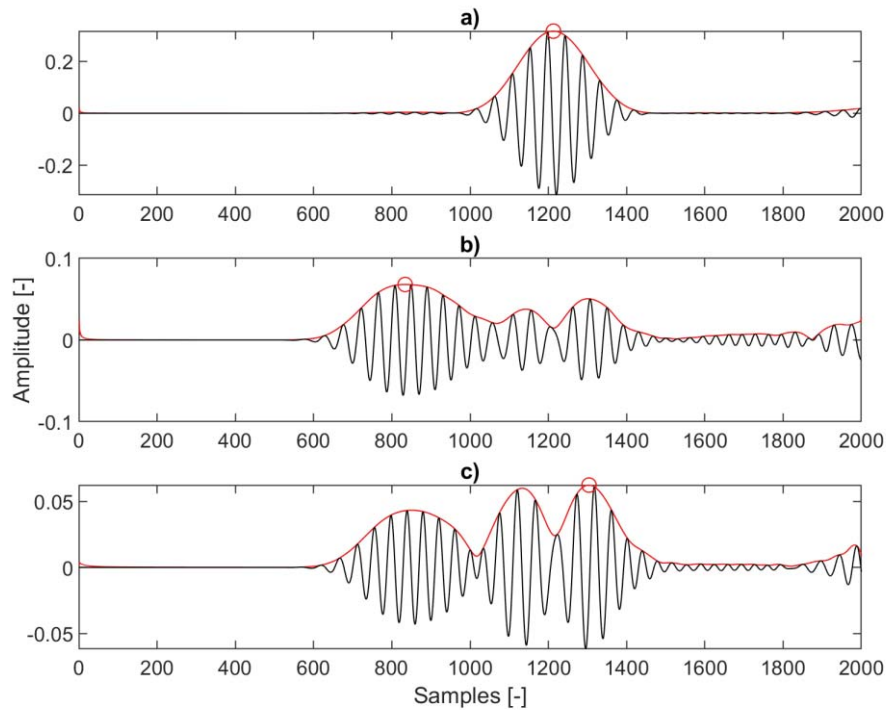


**Figure 3:** Examples of simulated wave propagation responses: (a) shear horizontal SH0 mode; (b) S0 Lamb wave mode; (c) A0 Lamb wave mode.

The directivity patterns of propagating waves can be seen in Figure 4. Identified maxima have been arranged in a polar plot, following the procedure described in Section 2.3. The results for the 200 and 617.5 kHz excitation frequency are presented in Figure 4. The excitation of 200 kHz frequency generates only two main lobes. This is in line with the second criterion described in Section 2.3. The excitation of 617.5 kHz frequency generates much narrower main lobes. In addition, side lobes can be also observed. The results show that commercial piezoceramic transducers that are used for shear wave generation in plates are also capable to generate Lamb waves, as expected. The results also demonstrate how important the geometry of the transducer and the excitation frequency when the shear horizontal SH0 wave needs to be optimised with respect to the maximum amplitude and directivity of wave propagation.

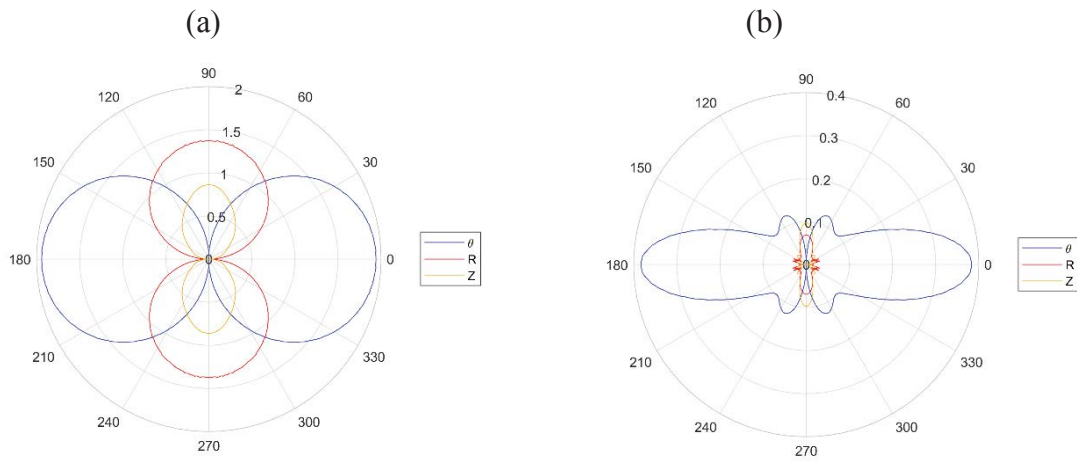


**Figure 4:** Numerical simulation of wave generation directivity patterns for different excitation frequencies.

#### 4 CONCLUSIONS

A thickness-shear  $d_{15}$  piezoceramic transducers has been modelled using finite elements. The major focus has been on the excitability and directivity of the fundamental shear horizontal SH0 mode.

The results show that commercial piezoceramic transducers that are used for shear wave generation in plates are also capable to generate Lamb waves. The results show that the geometry of the transducer and the excitation frequency significantly affects the generation of the fundamental shear horizontal mode in the plate.

Future work should focus more on the optimisation of geometry and excitation of transducers. Experimental work is also needed to validate numerical simulation results.



## REFERENCES

- [1] W.J. Staszewski, “Structural health monitoring using guided ultrasonic waves” in *Advances in Smart Technologies in Structural Engineering*, J. Holnicki-Szulc and C.A. Mota Soares, Eds., Berlin: Springer, 2004, pp. 117–162.
- [2] A.J. Croxford, P.D. Wilcox, B.W. Drinkwater and G. Konstantinidis, “Strategies for guided- wave structural health monitoring”, *Proceedings of the Royal Society*, vol. 463, pp. 2961–2981, 2007.
- [3] A. Raghavan A and C. Cesnik, “Review of guided-wave structural health monitoring”, *Shock and Vibration Digest*, pp. 39-116, 2007.
- [4] M. Castaigns, “SH ultrasonic guided waves for the evaluation of interfacial adhesion”, *Ultrasonics*, vol. 54(7), pp. 1760-1775, 2014.
- [5] P. Manogharan, X. Yu, Z. Fan and P. Rajagopal, “Interaction of shear horizontal bend (SH<sub>b</sub>) guided mode with defects”, *NDT & E International*, vol. 75, pp. 39-47, 2015.
- [6] C.J. Lissenden, “Nonlinear ultrasonic guided waves – principles for nondestructive evaluation”, *Journal of Applied Physics*, vol. 129, paper 021101, 2021.
- [7] M. Osika, A. Ziaja-Sujdak, R. Radecki, L. Cheng and W.J. Staszewski, “Nonlinear modes in shear horizontal wave propagation – analytical and numerical analysis”, *Journal of Sound and Vibration*, vol. 540, paper 117247, 2022.
- [8] H. Miao and F. Li, “Shear horizontal wave transducers for structural health monitoring and nondestructive testing: a review”, *Ultrasonics*, vol. 114, paper 106355, 2021.
- [9] R.B. Thompson, “Physical principles of measurements with EMAT transducers”, *Phys. Acoust.*, vol. 19, pp. 157–200, 1990.
- [10] A. Kamal and V. Giurgiutiu, “Shear horizontal wave excitation and reception with shear horizontal piezoelectric wafer active sensor (SH-PWAS)”, *Smart Materials and Structures*, vol. 23, paper 085019, 2014.
- [11] H. Miao, S. Dong and F. Li, “Excitation of fundamental shear horizontal wave by using face-shear (d36) piezoelectric ceramics. *Journal of Applied Physics*, vol. 119, paper 174101, 2016.



- [12] Q. Huan, H. Miao, and F. Li, “A nearly perfect omnidirectional shear-horizontal (SH) wave transducer based on a thickness poled, thickness-shear (d15) piezoelectric ring, *Smart Materials and Structures*, vol. 26, paper 08LT01, 2017.
- [13] V. Giurgiutiu. *Structural Health Monitoring with Piezoelectric Wafer Active Sensors*. Academic Press, 2007.
- [14] J.L. Rose. *Ultrasonic Guided Waves in Solid Media*. Cambridge: Cambridge University Press, 2014.
- [15] R.S. Dahiya and M. Valle. *Robotic Tactile Sensing – Technologies and System*. Dordrecht: Springer, 2013.
- [16] STEMiNC, [https://www.steminc.com/piezo/PZ\\_property.asp](https://www.steminc.com/piezo/PZ_property.asp), October 2021.